

Published in final edited form as:

*Brain*. 2015 November ; 138(Pt 11): 3159–3167. doi:10.1093/brain/awv257.

## Epileptogenic effects of NMDAR antibodies in a passive transfer mouse model

Sukhvir Wright<sup>1</sup>, Kevan Hashemi<sup>2</sup>, Lukasz Stasiak<sup>3</sup>, Julian Bartram<sup>3</sup>, Bethan Lang<sup>1</sup>, Angela Vincent<sup>#1</sup>, and A. Louise Upton<sup>#3</sup>

<sup>1</sup>Nuffield Department of Clinical Neurosciences, John Radcliffe Hospital, University of Oxford, Oxford, OX3 9DU, UK

<sup>2</sup>Open Source Instruments Inc, 130 Mount Auburn Street, Watertown, MA 02472, USA

<sup>3</sup>Department of Physiology, Anatomy and Genetics, University of Oxford, Oxford, OX1 3PT, UK

# These authors contributed equally to this work.

### Abstract

Most patients with *N*-methyl D-aspartate-receptor antibody encephalitis develop seizures but the epileptogenicity of the antibodies has not been investigated *in vivo*. Wireless electroencephalogram transmitters were implanted into 23 C57BL/6 mice before left lateral ventricle injection of antibody-positive (test) or healthy (control) immunoglobulin G. Mice were challenged 48 h later with a subthreshold dose (40 mg/kg) of the chemo-convulsant pentylenetetrazol and events recorded over 1 h. Seizures were assessed by video observation of each animal and the electroencephalogram by an automated seizure detection programme. No spontaneous seizures were seen with the antibody injections. However, after the pro-convulsant, the test mice ( $n = 9$ ) had increased numbers of observed convulsive seizures ( $P = 0.004$ ), a higher total seizure score ( $P = 0.003$ ), and a higher number of epileptic ‘spike’ events ( $P = 0.023$ ) than the control mice ( $n = 6$ ). At post-mortem, surprisingly, the total number of *N*-methyl D-aspartate receptors did not differ between test and control mice, but in test mice the levels of immunoglobulin G bound to the left hippocampus were higher ( $P < 0.0001$ ) and the level of bound immunoglobulin G correlated with the seizure scores ( $R^2 = 0.8$ ,  $P = 0.04$ ,  $n = 5$ ). Our findings demonstrate the epileptogenicity of *N*-methyl D-aspartate receptor antibodies *in vivo*, and suggest that binding of immunoglobulin G either reduced synaptic localization of *N*-methyl D-aspartate receptors, or had a direct effect on receptor function, which could be responsible for seizure susceptibility in this acute short-term model.

### Keywords

NMDAR; antibody; seizures; mouse electroencephalography

---

Correspondence to: Professor Angela Vincent, Nuffield Department of Clinical Neurosciences, Level 5/6 West Wing, John Radcliffe Hospital, Oxford, OX3 9DU, UK, [angela.vincent@ndcn.ox.ac.uk](mailto:angela.vincent@ndcn.ox.ac.uk).

### Conflicts of interest

A. V. B.L. and the University of Oxford hold patents and receive royalties and payments for antibody assays. K.H. is President of OpenSource Instruments and receives royalties for EEG transmitter sales. No other competing interests identified.

## Introduction

*N*-methyl D-aspartate receptor (NMDAR) antibody-mediated encephalitis commonly presents with features of psychiatric disturbance, cognitive problems, seizures and encephalopathy, usually followed by movement disorder, autonomic dysfunction, hypoventilation and coma (Dalmau *et al.*, 2007, 2008; Irani *et al.*, 2010). Despite the complexity and potential severity of the disease, eventually most patients who are diagnosed early and treated promptly with immunotherapy make a full or substantial recovery (Irani *et al.*, 2010; Titulaer *et al.*, 2013). It is widely thought that the NMDAR antibodies are pathogenic, with *in vitro* and *in vivo* experiments showing loss of NMDAR, most evident in the hippocampus (Hughes *et al.*, 2010; Planaguma *et al.*, 2014), and demonstrated also in patient brain tissue post-mortem (Dalmau *et al.*, 2007). Mice infused with NMDAR antibody-positive CSF over 14 days showed cognitive and behavioural impairment (Planaguma *et al.*, 2014), but other clinical features of the disease have not been demonstrated in animal models. Seizures are frequently observed in patients and NMDAR antibodies have also been reported in a few epilepsy patients without encephalitis (Niehusmann *et al.*, 2009; Quek *et al.*, 2012; Brenner *et al.*, 2013; Suleiman *et al.*, 2013). Here we examined the effects of intra cerebral-ventricular injections of NMDAR antibodies in mice using wireless EEG telemetry.

## Materials and methods

### Purification of patient IgG

Immunoglobulin G (IgG) was prepared using Protein G Sepharose beads (Sigma; see Supplementary material) from plasma obtained, with informed consent, at plasmapheresis, from three female NMDAR antibody-positive patients (Patients 1–3) with neuropsychiatric features, movement disorder, and reduced levels of consciousness. Control IgG was purified from two healthy individuals (Control subjects 1 and 2). The purified IgGs were tested for binding to rodent brain tissue sections and live hippocampal neurons and were endpoint titrated on a live cell-based assay for NMDAR antibodies (as in Irani *et al.*, 2010).

### Implantation of telemetric transmitters

C57BL/6 female mice (aged 8–10 weeks, weighing 18–22 g) were housed (Supplementary material) and examined according to ARRIVE guidelines ([www.nc3rs.org.uk/arrive-guidelines](http://www.nc3rs.org.uk/arrive-guidelines)) with all analyses performed with the observer blinded to the injected IgG. Under isoflurane anaesthesia, mice were placed in a stereotaxic frame and a 2 cm incision made caudally over the skull surface. A subcutaneous pocket was formed over the right flank by blunt tissue dissection, and the transmitter (Open Source Instruments, A3019A, weight 2.4 g) inserted into it (Fig. 1A), with the rubber-ensheathed electrode wires and attached screws left anteriorly exposed prior to fixation to the skull surface. Two holes were drilled through the skull at coordinates 1 mm lateral and 1 mm caudal from bregma (to leave enough space for subsequent intracerebroventricular injections). Electrode screws were fixed into the drilled holes with dental cement to hold them in place. Mash and a heat pad were provided during the initial recovery. The animals returned to their home cage for a minimum of 5 days before any further procedures. To monitor welfare, daily records of weight, appearance,

wound healing, spontaneous and provoked behaviour were kept throughout the experimental period.

### **Stereotaxic injection of human IgG**

Mice were placed in a stereotaxic frame under isoflurane anaesthesia, and the skull surface exposed. A single burr hole was made 1 mm left lateral and 0.45 mm caudal from bregma. Eight microlitres of purified IgG from either NMDAR antibody-positive or healthy controls was slowly injected over 20 min into the left cerebral ventricle using a Hamilton syringe with a 33 gauge needle inserted at a depth of  $-1.85$  mm from dura. Three hundred nanolitres of fluorescent beads (Lumafuor Inc.) were simultaneously injected to identify the location post-mortem (Fig. 1B). After the IgG injection, the Hamilton syringe was left in place for 5 min to allow for diffusion and then withdrawn slowly. The skin was sutured and the animal was allowed to recover in a warm chamber before being replaced in its home cage.

### **Collection and analysis of EEG data**

The mice were housed in a Faraday cage with an aerial to collect the EEG signals. Transmitter signals were continuously recorded in the freely moving mice using Neuroarchiver software (Open Source Instruments) for up to 28 days (Chang *et al.*, 2011). The raw EEG was analysed by observing the EEG trace during playback of the archived files alongside the Event Classifier application in Neuroarchiver. Two methods were used for seizure detection in the EEG: power band analysis to calculate changes in power of different frequency wavelength bands and an automated epileptic event detection programme. The power of oscillation of the EEG trace at different frequencies was calculated by subjecting it to a Fourier transform and then dividing it up into predefined frequency bands (delta 1–4 Hz, theta 4–8 Hz, alpha 8–12 Hz, beta 12–30 Hz, low gamma 30–50 Hz, high gamma 50–70 Hz, high frequency 70–120 Hz), using the Power Band Average script provided by OpenSource Instruments.

For automated epileptic event detection, video-EEG matching was first used to identify EEG events of interest associated with an observed behaviour/seizure. The Event Classifier (OpenSource Instruments) was then used to classify the short segments of EEG according to several metrics enabling similar events to cluster together when plotted according to the metrics. This generated a library of distinctive and potentially pathological events that allowed fast identification of abnormal EEG events by automated comparison to the library ([http://www.opensourceinstruments.com/Electronics/A3018/Seizure\\_Detection.html](http://www.opensourceinstruments.com/Electronics/A3018/Seizure_Detection.html)) (Wykes *et al.*, 2012).

### **Seizure induction**

To test seizure susceptibility, 40 mg/kg dose of pentylenetetrazol (PTZ) was given intraperitoneally (Weiergraber *et al.*, 2006; Luttjohann *et al.*, 2009) and the mice were observed for 60 min while recording and observing seizure events (Supplementary Table 1). Frequency of seizures, latency to onset of convulsive seizures and total seizure score were recorded; the latter was calculated at the end of the 60-min observation period, with a score of 2 or 3 given for each stage 2 or 3 seizure. The observation period was video recorded to allow subsequent video-EEG matching of observed events with EEG signatures.

## Analysis of brain tissue

Immediately after the observation period, the mice were perfused with phosphate-buffered saline (PBS), and the left brain hemispheres removed, flash frozen in isopentane and stored at  $-80^{\circ}\text{C}$ . Brain sections were cut at  $12\ \mu\text{m}$  thickness using a Leica CM1900 cryostat at  $-18^{\circ}\text{C}$ . These were used for determination of the amount of IgG bound *in situ*, analysis of both intracellular and surface NMDAR, and terminal deoxynucleotidyl transferase dUTP nick end labelling (TUNEL) staining for apoptosis. The right hemisphere was post-fixed before freezing and sectioning for c-fos expression. Details of TUNEL and c-fos expression are provided in the Supplementary material.

## Measurement of IgG bound and NMDA receptors in mouse brains

For determination of human IgG bound *in vivo*, the unfixed sections were rinsed gently with PBS then blocked with 10% normal goat serum (NGS) for 45 min before incubation in anti-human IgG Alexa Fluor<sup>®</sup> 488 at 1:1000 (A11013; Invitrogen) overnight at  $4^{\circ}\text{C}$ . Sections were washed and mounted with aqueous mounting medium containing DAPI.

For detection of total NMDAR we used an antibody to the obligate subunit NR1. The sections were fixed for 5 min with 3% formaldehyde and washed in PBS, then blocked and permeabilized using 1% Triton<sup>™</sup> in PBS with 10% NGS for 45 min. The primary antibody [purified mouse anti-NR1 (raised against intracellular sequence amino acid residues 660–811), no. 556308, BD Pharmingen] was incubated overnight at  $4^{\circ}\text{C}$  at a dilution of 1:250 in PBS with 5% NGS. Sections were then incubated in anti-mouse IgG Alexa Fluor<sup>®</sup> 488 at 1 in 1000 (A11001; Invitrogen) for 1 h, washed in PBS three times, and mounted as above.

To determine the surface NMDAR, further sections were blocked with 10% NGS and incubated with human NMDAR antibody-positive CSF at 1:20 overnight at  $4^{\circ}\text{C}$  (as in Planaguma *et al.*, 2014). The next day, slides were washed and incubated with Alexa Fluor<sup>®</sup> 488 anti-human IgG for 1 h at room temperature and processed as above. To determine the proportion of this NMDAR that was not already bound *in vivo* by IgG, we subtracted the IgG bound fluorescence detected in adjacent serial sections.

All sections were photographed from coded slides, and analysed with ImageJ software (open source software) as described in the Supplementary material.

## Statistics

Data were analysed using GraphPad Prism 6. Non-categorical data were analysed by the Mann-Whitney test. The correlation between seizure score and levels of bound IgG was assessed by linear correlation.

## Results

The purified NMDAR antibody-positive IgG preparations (concentrations 8–40 mg/ml), but not the controls (both at 25 mg/ml), bound with high titres throughout the molecular cell layer of the hippocampus on rodent sagittal brain sections, to live cultured hippocampal neurons, and in the NMDAR cell-based assay (data not shown).

### Experiment 1: Intracerebroventricular injection of IgG

Eight C57BL/6 female mice were implanted with EEG transmitters (Day 1) and injected intracerebroventricularly (Fig. 1A and B) with IgG from NMDAR antibody Patient 1 (four mice) and healthy Control subject 1 (four mice) on Day 7 and again on Day 14 post-implantation. No seizure activity was witnessed and power band analysis of the continuous EEG recording revealed no increases in average power in any frequency bands that would indicate spontaneous seizure activity throughout the 21 days of observations (Supplementary Fig. 1A–C). A small increase in delta power (1–4 Hz) was observed in both groups after the second injection, with no difference between the patient and healthy control groups.

### Experiment 2: Intracerebroventricular injection of IgG with PTZ seizure induction

As C57BL/6 mice are known to be seizure-resistant (Ferraro *et al.*, 1998, 1999), we challenged the IgG-injected mice with the seizure-inducing compound PTZ at a subthreshold concentration normally used for chemical kindling (Dhir *et al.*, 2005; Rajabzadeh *et al.*, 2012). Preliminary experiments (data not shown) confirmed that 40 mg/kg did not lead to seizures (stage 2) in naïve C57BL/6 mice ( $n = 2$ ). Fifteen mice were implanted with the telemetry devices and 7 days later given intracerebroventricular injections of either NMDAR antibody IgG from Patients 1, 2 or 3 (three mice for each) or healthy Control subjects 1 and 2 IgG (three mice for each). No spontaneous seizures were identified in the 48 h after the intracerebroventricular injections. At that time, 40 mg/kg PTZ was injected intraperitoneally, and mice were videoed for 1 h before culling.

PTZ injection produced some convulsive seizures in all mice (Supplementary Videos 1 and 2), which were manually scored by a blinded observer. Seizure number was higher in the NMDAR antibody-injected mice [median seizures/mouse (range) 10 (2–33),  $n = 9$ ] compared to the healthy control IgG-injected mice [median seizures/mouse (range) 3 (1–5),  $n = 6$ ; Mann Whitney  $P = 0.004$ ; Fig. 1C and D]. There was a trend towards a shorter latency to the first convulsive seizure in the NMDAR antibody IgG-injected mice [median value 2.3 min (range 0.97–6.18 min) versus 7.45 min (range 2.3–17.75 min),  $P = 0.09$ ] although the total numbers of stage 2 seizures were not different [ $7.6 \pm 2.8$  (0–23) versus  $2.5 \pm 0.8$  (0–5),  $P = 0.5$ ]. However, the more severe stage 3 seizures were seen in all the NMDAR antibody IgG-injected mice compared to only three of six of the healthy control IgG-injected mice ( $P = 0.04$ ), and the number of stage 3 seizures per mouse was higher in the NMDAR antibody IgG-injected mice [mean  $\pm$  standard error of the mean (SEM) (range)  $7.7 \pm 2.8$  (1–29)] compared to the healthy control IgG-injected group [ $0.83 \pm 0.4$  (0–2);  $P = 0.003$ ; Fig. 1E]. Finally, a higher total seizure score per mouse was seen in the NMDAR antibody IgG-injected animals ( $38.3 \pm 9.8$  versus  $7.5 \pm 1.67$ ; Fig. 1F;  $P = 0.003$ ). The individual results are shown in Table 1.

### Automatic event detection

Although power band analysis revealed no differences in the EEG between the two groups (see above), rare individual seizure events may be lost in the averaging. An Event Classification Processor was used to create a library of specific EEG events of interest for screening the EEG data for discrete seizures. Using the concurrent video and EEG from the 60 min following the injection of PTZ, segments of EEG were classified according to six

metrics and manually assigned to categories for the library (Fig. 2A). These included ‘spikes’, which occurred with convulsive seizures and ‘headshakes’.

Using this library, EEG data from Experiments 1 and 2 were analysed and the frequency of each event type counted. The average number of daily headshakes tended to increase with the number of surgical procedures in both groups (Supplementary Fig. 1D). Epileptic ‘spike’ events were not seen in the animals in Experiment 1, or before PTZ seizure induction in Experiment 2, but after PTZ the spike events were more numerous in NMDAR antibody IgG-injected mice than in healthy control IgG-injected mice ( $P = 0.02$ ; Fig. 2B and C). Individual data are given in Table 1.

### Analysis of brain tissue

To examine the effects of NMDAR antibody IgG on cell excitation and cell death, in Experiment 2, mice were sacrificed immediately following PTZ injection, 49 h after the IgG injections. Brain tissue from mice in each group was processed for immunostaining for c-fos (NMDAR antibody IgG,  $n = 3$ ; healthy control IgG,  $n = 3$ ) and TUNEL staining (NMDAR antibody IgG,  $n = 2$ ; healthy control IgG,  $n = 2$ ). Five mice had c-fos expression in cortex, but one healthy control IgG-injected mouse (E12), with only stage 2 (partial) seizures was negative. The number of c-fos-positive cells did not differ between the two groups, and apoptosis was not seen in areas of NMDAR antibody IgG binding (Supplementary Fig. 2). One healthy control IgG-injected mouse showed detectable TUNEL staining in the needle track (not shown); no other TUNEL staining was observed.

### Identification of IgG bound and surface NMDAR

To determine whether seizure scores were related to the IgG bound, unfixed, lightly washed, mouse brain tissue was examined for bound human IgG using fluorescent anti-human IgG on multiple sections across the hippocampi. Human IgG was easily detected in the hippocampi of NMDAR antibody IgG-injected mice (Fig. 3A), with little in the healthy control IgG-injected tissue (Fig. 3B), or in other brain regions where NMDAR expression is lower (i.e. cerebellum and cortex, data not shown). There was variability in the IgG fluorescence intensity across the hippocampi but overall the bound IgG was higher in NMDAR- antibody injected mice in each of the three hippocampal regions analysed, particularly in the CA3 (Fig. 3C), and on pooling the data for all three regions ( $P < 0.001$ ). The seizure scores in NMDAR antibody injected mice correlated with the amount of IgG bound ( $n = 5$ ) (Fig. 3D;  $R^2 = 0.8$ ,  $P = 0.04$ ), with a similar trend for the CA3 regions only ( $R^2 = 0.7$ ,  $P = 0.07$ , data not shown). The individual results are shown in Table 1.

To see if the bound IgG was associated with loss of surface NMDAR, we first tested binding of the only available commercial anti-NR1 antibody, which binds an intracellular NMDAR epitope on the NR1 subunit, and required tissue permeabilization; the results were not different between NMDAR antibody IgG- and healthy control IgG-injected brains (Fig. 3E and F). We then used highly positive NMDAR antibody CSF to identify surface NMDAR (as in Planaguma *et al.*, 2014). In this situation, the secondary antibody also detected the IgG that had bound *in vivo*. In brains from four NMDAR antibody injected mice (E15, E20, E23, E19) and two healthy control IgG-injected mice (E14, E21), the total NMDAR (e.g. IgG



bound *in vivo* and that bound *ex vivo*; Fig. 3G) were measured in parallel and were not different between test and control hippocampi (Fig. 3H). However, as determined on adjacent sections for direct comparison (Supplementary Fig. 3), a proportion of the surface NMDAR was already bound by human IgG (Fig. 3H) with, consequently, a 19.7% reduction in the number of NMDAR free of bound IgG ( $P = 0.035$ , Fig. 3H).

## Discussion

Demonstrating the pathogenicity of specific antibodies in CNS disease has proved difficult and transfer of clinical features of NMDAR antibody encephalitis to mice has so far been limited to cognitive defects and altered behaviour (Planaguma *et al.*, 2014). To examine whether NMDAR antibodies were epileptogenic, we observed seizure events after subthreshold injection of PTZ in EEG transmitter-implanted mice, and produced an ‘event classifier’ suitable for automatic screening of the EEG recordings. Although a single injection of purified IgG from NMDAR antibody patients did not produce spontaneous seizures, the number and severity of seizures following the subthreshold dose of PTZ injection was increased in the NMDAR antibody IgG-injected mice. This effect correlated with the quantity of IgG bound to the hippocampus *in vivo*, and with a 19.7% reduction in non-IgG bound surface NMDARs, demonstrating a likely role for the NMDAR antibody IgG.

The purified IgG was injected into the lateral ventricle to circumvent the blood-brain barrier and increase parenchymal antibody binding. As rodent CSF is recirculated up to 12 times a day (Chiu *et al.*, 2012), a single 8  $\mu$ l bolus of purified IgG might not have produced adequate tissue penetration, but on examination 49 h after the injection, there was clear evidence of IgG bound in the hippocampus, correlating with the seizure scores. Planaguma *et al.* (2014) found NMDAR antibody IgG bound *in vivo* after 5 days of osmotic pump infusions with 12  $\mu$ l pooled CSF per day, but only detected cognitive/behavioural changes from Day 10. This suggests that there may be some advantages in a single injection of high concentration NMDAR antibody IgG, particularly to look at the earliest events in the disease process. A comparison of the methods can be found in Supplementary Table 2.

Previous studies showed that internalization by divalent antibodies results in loss of NMDAR from the hippocampus and on cultured neurons (Hughes *et al.*, 2010; Moscato *et al.*, 2014). Ideally one would use a commercial antibody to measure the surface NMDAR expression in the tissue *ex vivo*, but only an intracellular antibody was available and this showed no differences between the two groups of mice. Instead we used patient CSF to measure the total surface NMDAR *ex vivo* but again found no difference. By contrast, Planaguma *et al.* (2014) using patient CSF antibody binding and an automated spot-detection algorithm on 3D confocal images, found reductions in total and synaptic NMDAR after 14 days of patient antibody infusion. The discrepancy between our results and theirs may reflect the difference in the analytical methods and durations of treatment between the two studies.

Nevertheless, the lack of a change in total NMDAR raises questions regarding the pathogenic mechanism underlying seizure susceptibility in this study. One possibility is that

the NMDAR with IgG bound *in vivo* had altered function. Several studies report an acute action of the NMDAR antibodies including an increase in the extrasynaptic concentration of glutamate within 30 min of an infusion of NMDAR antibodies *in vivo* into the CA1 area of rats (Manto *et al.*, 2010), suppression of long-term potentiation induction in *ex vivo* mouse hippocampal slices following a 5-min application of NMDAR antibodies (Zhang *et al.*, 2012), and acute suppression of global activity in an *in vitro* neuronal network of dissociated primary rat cortical neurons, as recorded by the microelectrode (MEA) system after application of NMDAR antibody CSF (Jantzen *et al.*, 2013). In contrast to these studies, Moscato *et al.* (2014) found a lack of effect of NMDAR antibodies on NMDAR-mediated current amplitudes in hippocampal neurons when treated for only 30 min, as opposed to the dramatic reduction resulting from 24 h of treatment when the NMDARs are internalized. Given the reduction of NMDAR expression seen in patients post-mortem, loss of NMDAR by antibody-mediated internalization is likely to be a major contributor to NMDAR hypofunction, but direct pharmacological blockade of the receptor remains a possibility, particularly in this acute model. Indeed, the correlation we found between IgG bound and seizure scores would support this hypothesis.

Another possibility is that the NMDAR with bound IgG was mainly at extrasynaptic sites, where it would be in the process of internalization (as in Mikasova *et al.* 2012), whereas the non-IgG bound NMDAR might be mainly synaptic where the 19.7% reduction could be responsible for the epileptogenic effects seen. It is also possible that the change in NMDAR that underlies seizure susceptibility in this model is restricted to a relatively small but critical, population of cells. Indeed, there are precedents for loss of NMDAR on inhibitory neurons causing seizures. In the NR1 hypomorphic mice, where 80% of NMDAR is lost, all mice experience lethal seizures at a low 20 mg/kg dose of kainic acid compared to controls; these mice had altered excitatory–inhibitory signalling with selective disruption of parvalbumin-positive interneurons and pyramidal cell excitability (Gandal *et al.*, 2012). The parvalbumin interneurons are more sensitive to NMDAR antagonists than pyramidal neurons (Grünze *et al.*, 1996; Li *et al.*, 2002), and it is possible that NMDAR on inhibitory interneurons are more susceptible/accessible to NMDAR antibodies or are preferentially targeted in our model. On the other hand, while preferential binding to inhibitory interneurons has not been shown, a reduction in GABAergic synaptic density onto excitatory neurons was seen within 24 h of NMDAR antibody application *in vitro* (Moscato *et al.*, 2014). Loss of pyramidal cell NMDAR has also been shown to affect cortical excitability. Mutant mice lacking NMDAR in the hippocampal CA3 pyramidal neurons were more susceptible to kainate-induced seizures, and pharmacological blockade of CA3 NMDAR in adult wild-type mice produced similar results (Fukushima *et al.*, 2009). This suggests a role for NMDAR in exerting negative control over the CA3 recurrent network, and hence network excitability *in vivo*, and may offer an alternative (or perhaps additional) hypothesis for the seizure susceptibility observed here.

These results, and those of Planaguma *et al.* (2014) confirm the pathogenicity of NMDAR antibodies and show that they increase seizure susceptibility and cause cognitive and behavioural deficits, but as yet neither model has shown the characteristic movement disorder that usually occurs later in the disease (Irani *et al.*, 2010). Further work, including *ex vivo* and *in vitro* electrophysiology, is required to determine the relative contribution of



acute effects of NMDAR antibodies on receptor function versus internalization, as well as to examine the effect on specific cell populations within hippocampal neuronal circuits. Such studies should increase our understanding of the roles of NMDAR in health and disease.

## Supplementary Material

Refer to Web version on PubMed Central for supplementary material.

## Acknowledgements

We are very grateful to Prof Matthew Walker for advice, to Dr Philippa Pettingill for providing Patient 1 NMDAR antibody-positive IgG, Drs Teresa Moloney and Leslie Jacobson, and Ms Linda Clover for assistance with immunocytochemistry and immunohistochemistry analysis, and to Joost Heeroma who assisted with preliminary EEG analysis.

### Funding

This work was supported by a Clinical Research Training Fellowship from the Wellcome Trust/University of Oxford Grant code HMRVOW0 (S.W.), and by the National Institute for Health Research Oxford Biomedical Research Centre based at Oxford University Hospitals NHS Trust and the University of Oxford (A.V.), and the Wellcome Trust funded OXION initiative at the Department of Physiology, Anatomy and Genetics, University of Oxford (L.U., J.B., L.S.).

## Abbreviations

<b>IgG</b>	immunoglobulin G
<b>NMDAR</b>	<i>N</i> -methyl D-aspartate-receptor
<b>PTZ</b>	pentylentetrazol

## References

- Brenner T, Sills GJ, Hart Y, Howell S, Waters P, Brodie MJ, et al. Prevalence of neurologic autoantibodies in cohorts of patients with new and established epilepsy. *Epilepsia*. 2013; 54:1028–35. [PubMed: 23464826]
- Chang P, Hashemi KS, Walker MC. A novel telemetry system for recording EEG in small animals. *J Neurosci Methods*. 2011; 201:106–15. [PubMed: 21820010]
- Chiu C, Miller MC, Caralopoulos IN, Worden MS, Brinker T, Gordon ZN, et al. Temporal course of cerebrospinal fluid dynamics and amyloid accumulation in the aging rat brain from three to thirty months. *Fluids Barriers CNS*. 2012; 9:3. [PubMed: 22269091]
- Dalmau J, Tuzun E, Wu HY, Masjuan J, Rossi JE, Voloschin A, et al. Paraneoplastic anti-N-methyl-D-aspartate receptor encephalitis associated with ovarian teratoma. *Ann Neurol*. 2007; 61:25–36. [PubMed: 17262855]
- Dalmau J, Gleichman AJ, Hughes EG, Rossi JE, Peng X, Lai M, et al. Anti-NMDA-receptor encephalitis: case series and analysis of the effects of antibodies. *Lancet Neurol*. 2008; 7:1091–8. [PubMed: 18851928]
- Dhir A, Naidu PS, Kulkarni SK. Effect of naproxen, a non-selective cyclo-oxygenase inhibitor, on pentylentetrazol-induced kindling in mice. *Clin Exp Pharmacol Physiol*. 2005; 32:574–84. [PubMed: 16026518]
- Ferraro TN, Golden GT, Snyder R, Laibinis M, Smith GG, Buono RJ, et al. Genetic influences on electrical seizure threshold. *Brain Res*. 1998; 813:207–10. [PubMed: 9824700]
- Ferraro TN, Golden GT, Smith GG, St Jean P, Schork NJ, Mulholland N, et al. Mapping loci for pentylentetrazol-induced seizure susceptibility in mice. *J Neurosci*. 1999; 19:6733–9. [PubMed: 10436030]

- Fukushima F, Nakao K, Shinoe T, Fukaya M, Muramatsu S, Sakimura K, et al. Ablation of NMDA receptors enhances the excitability of hippocampal CA3 neurons. *PloS One*. 2009; 4:e3993. [PubMed: 19142228]
- Gandal MJ, Sisti J, Klook K, Ortinski PI, Leitman V, Liang Y, et al. GABAB-mediated rescue of altered excitatory-inhibitory balance, gamma synchrony and behavioral deficits following constitutive NMDAR-hypofunction. *Transl Psychiatry*. 2012; 2:e142. [PubMed: 22806213]
- Grunze HC, Rainnie DG, Hasselmo ME, Barkai E, Hearn EF, McCarley RW, et al. NMDA-dependent modulation of CA1 local circuit inhibition. *J Neurosci*. 1996; 16:2034–43. [PubMed: 8604048]
- Hughes EG, Peng X, Gleichman AJ, Lai M, Zhou L, Tsou R, et al. Cellular and synaptic mechanisms of anti-NMDA receptor encephalitis. *J Neurosci*. 2010; 30:5866–75. [PubMed: 20427647]
- Irani SR, Bera K, Waters P, Zuliani L, Maxwell S, Zandi MS, et al. N-methyl-D-aspartate antibody encephalitis: temporal progression of clinical and paraclinical observations in a predominantly non-paraneoplastic disorder of both sexes. *Brain*. 2010; 133(Pt 6):1655–67. [PubMed: 20511282]
- Jantzen SU, Ferrea S, Wach C, Quasthoff K, Illes S, Scherfeld D, et al. *In vitro* neuronal network activity in NMDA receptor encephalitis. *BMC Neurosci*. 2013; 14:17. [PubMed: 23379293]
- Li Q, Clark S, Lewis DV, Wilson WA. NMDA receptor antagonists disinhibit rat posterior cingulate and retrosplenial cortices: a potential mechanism of neurotoxicity. *J Neurosci*. 2002; 22:3070–80. [PubMed: 11943810]
- Luttjohann A, Fabene PF, van Luijtelaar G. A revised Racine's scale for PTZ-induced seizures in rats. *Physiol Behav*. 2009; 98:579–86. [PubMed: 19772866]
- Manto M, Dalmau J, Didelot A, Rogemond V, Honnorat J. In vivo effects of antibodies from patients with anti-NMDA receptor encephalitis: further evidence of synaptic glutamatergic dysfunction. *Orphanet J Rare Dis*. 2010; 5:31. [PubMed: 21110857]
- Mikasova L, De Rossi P, Bouchet D, Georges F, Rogemond V, Didelot A, et al. Disrupted surface cross-talk between NMDA and Ephrin-B2 receptors in anti-NMDA encephalitis. *Brain*. 2012; 135:1606–21. [PubMed: 22544902]
- Moscato EH, Peng X, Jain A, Parsons TD, Dalmau J, Balice-Gordon RJ. Acute mechanisms underlying antibody effects in anti-N-methyl-D-aspartate receptor encephalitis. *Ann Neurol*. 2014; 76:108–19. [PubMed: 24916964]
- Niehusmann P, Dalmau J, Rudlowski C, Vincent A, Elger CE, Rossi JE, et al. Diagnostic value of N-methyl-D-aspartate receptor antibodies in women with new-onset epilepsy. *Arch Neurol*. 2009; 66:458–64. [PubMed: 19364930]
- Planaguma J, Leyboldt F, Mannara F, Gutierrez-Cuesta J, Martin-Garcia E, Aguilar E, et al. Human N-methyl D-aspartate receptor antibodies alter memory and behaviour in mice. *Brain*. 2014; 138:94–109. [PubMed: 25392198]
- Quek AM, Britton JW, McKeon A, So E, Lennon VA, Shin C, et al. Autoimmune epilepsy: clinical characteristics and response to immunotherapy. *Arch Neurol*. 2012; 69:582–93. [PubMed: 22451162]
- Rajabzadeh A, Bideskan AE, Fazel A, Sankian M, Rafatpanah H, Haghiri H. The effect of PTZ-induced epileptic seizures on hippocampal expression of PSA-NCAM in offspring born to kindled rats. *J Biomed Sci*. 2012; 19:56. [PubMed: 22651102]
- Suleiman J, Wright S, Gill D, Brilot F, Waters P, Peacock K, et al. Autoantibodies to neuronal antigens in children with new-onset seizures classified according to the revised ILAE organization of seizures and epilepsies. *Epilepsia*. 2013; 54:2091–100. [PubMed: 24151870]
- Titulaer MJ, McCracken L, Gabilondo I, Armangue T, Glaser C, Iizuka T, et al. Treatment and prognostic factors for long-term outcome in patients with anti-NMDA receptor encephalitis: an observational cohort study. *Lancet Neurol*. 2013; 12:157–65. [PubMed: 23290630]
- Weiergraber M, Henry M, Krieger A, Kamp M, Radhakrishnan K, Hescheler J, et al. Altered seizure susceptibility in mice lacking the Ca(v)2.3 E-type Ca<sup>2+</sup> channel. *Epilepsia*. 2006; 47:839–50. [PubMed: 16686648]
- Wykes RC, Heeroma JH, Mantoan L, Zheng K, MacDonald DC, Deisseroth K, et al. Optogenetic and potassium channel gene therapy in a rodent model of focal neocortical epilepsy. *Sci Transl Med*. 2012; 4:161ra52.

Zhang Q, Tanaka K, Sun P, Nakata M, Yamamoto R, Sakimura K, et al. Suppression of synaptic plasticity by cerebrospinal fluid from anti-NMDA receptor encephalitis patients. *Neurobiol Dis.* 2012; 45:610–15. [PubMed: 22008231]

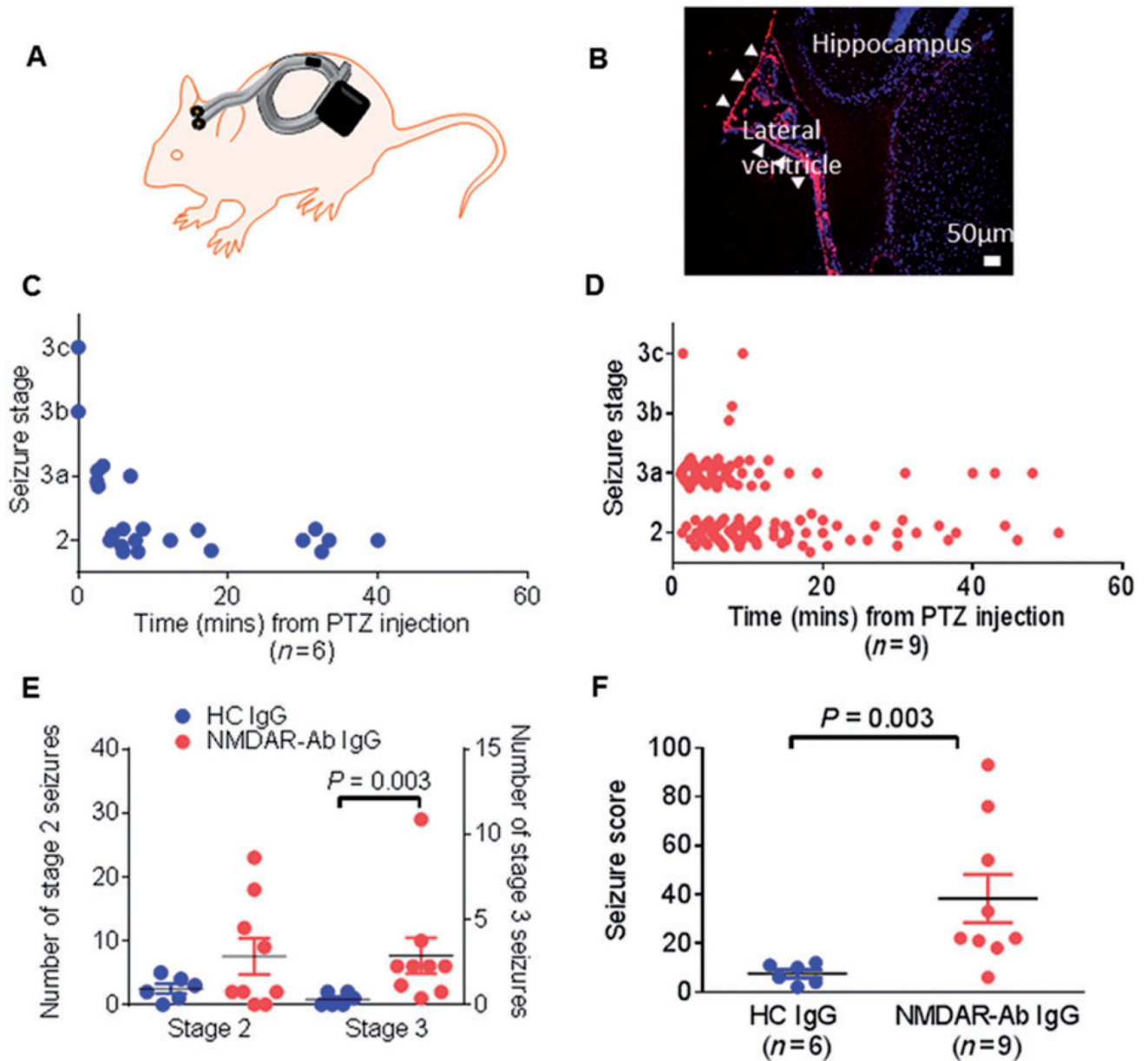


**Figure 1. Experimental technique and epileptogenic effects of a single injection of NMDAR antibodies.**

(A) Diagram of placement of subcutaneous wireless transmitter in mice. (B) Fluorescent beads (red) lining the lateral ventricle show successful needle placement of the IgG injection (hippocampal fields indicated by DAPI staining in blue). (C and D) Group ethograms of all healthy control IgG (C,  $n = 6$ ), and NMDAR antibody IgG (D,  $n = 9$ ) injected mice following PTZ injection showing the times of different seizure events over the 60-min period before culling (see Supplementary Videos 1 and 2 for examples of stage 2 and stage 3 seizures, respectively). (E) Stage 3 convulsive seizures but not stage 2 seizures were more frequent in the NMDAR antibody IgG-injected mice following PTZ ( $P = 0.003$ ). (F) The average score calculated for the 60-min observation period following PTZ was higher for

NMDAR antibody IgG- than healthy control IgG-injected mice ( $P = 0.003$ ). Error bars are mean  $\pm$  SEM. HC = Healthy control; NMDAR-Ab = NMDAR antibody.

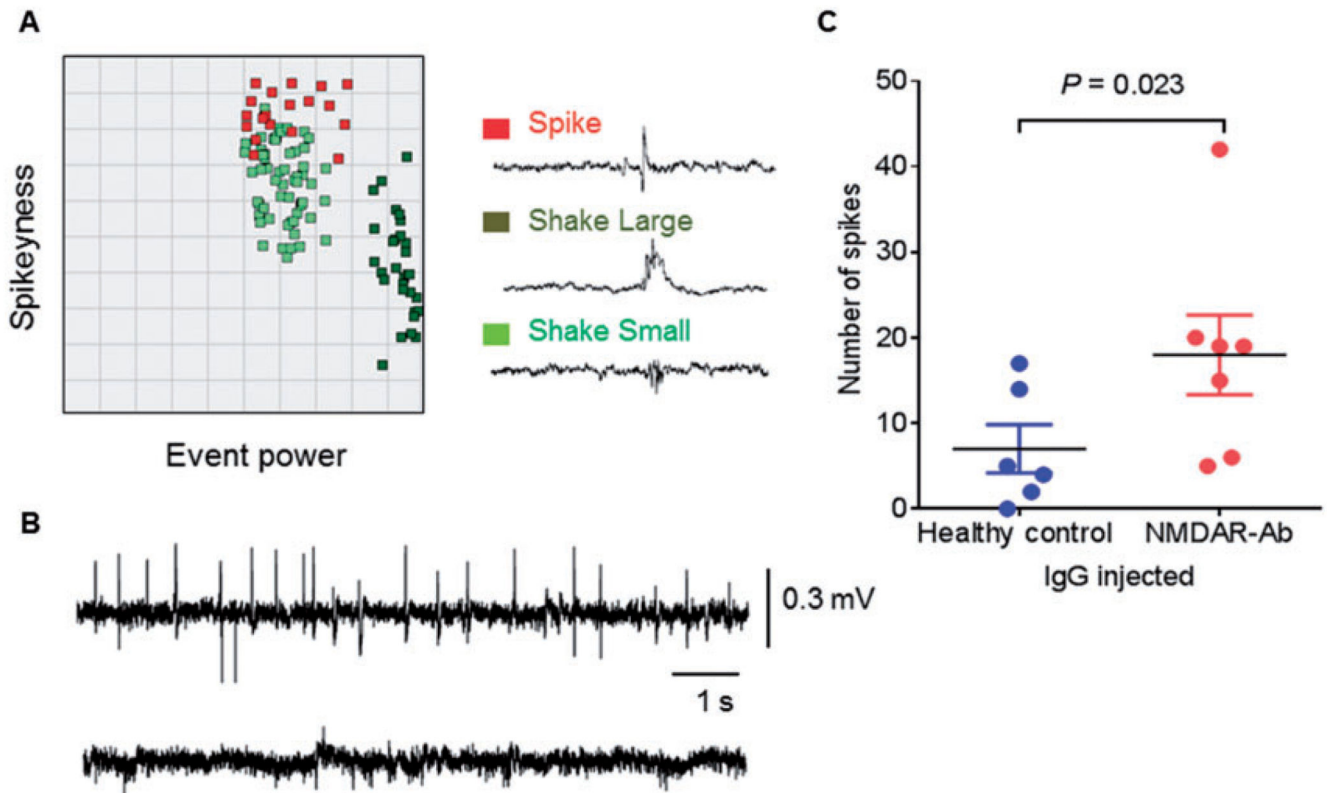


**Figure 2. EEG telemetry and analysis.**

(A) 2D representation of the event library with corresponding examples of library events. One second epochs of EEG on the right are defined by six separate metrics (calculated characteristics of the EEG waveform), two of which are indicated on the axes. Each small square (red/light green/dark green) represents an event as defined by six separate metrics and confirmed by visual inspection of the EEG and accompanying video. Similar events cluster together when plotted. ‘Spike’ was seen with a convulsive seizure, ‘Shake large’ and ‘Shake small’ were both seen with headshakes and needed to be differentiated from epileptiform activity. This library was used to screen EEG data by automated computer detection. (B) A representative EEG of an NMDAR antibody-injected mouse post-PTZ shows a number of ‘spikes’ corresponding to convulsive seizures (*upper trace*), compared to the EEG of a healthy control IgG-injected mouse, which has minimal spike activity (*lower trace*). (C) When analysed using the computer-based event detection program and blinded observer verification, the number of spikes seen in the hour following PTZ injection was greater in the NMDAR antibody ( $n = 7$ ; data from two mice were excluded because there was significant signal drop-out/loss during the PTZ seizure induction hour) compared to the healthy control IgG ( $n = 6$ ) injected mice ( $P = 0.023$ , Mann-Whitney). Results are mean  $\pm$  SEM.



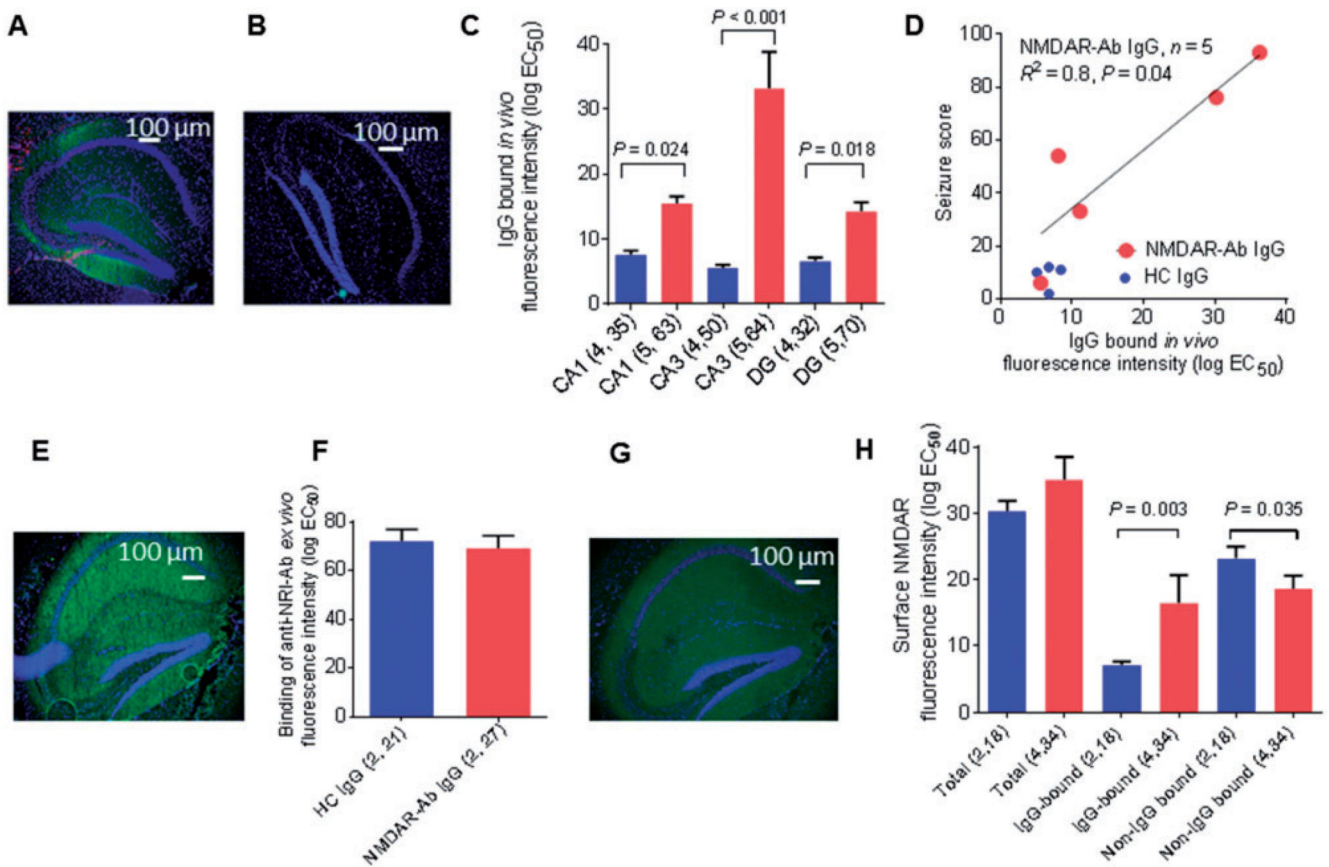


**Figure 3. Detection of bound human IgG and NMDAR expression in hippocampi *ex vivo*.**

(A) Human IgG injected *in vivo* was detected post-mortem in NMDAR antibody IgG-injected mice with anti-human IgG merged with the nuclear stain DAPI. The typical pattern of NMDAR antibody in the molecular cell layer with sparing of the granule cell layer was found. (B) Only low levels of IgG were found in the hippocampi of healthy control IgG-injected mice. (C) Bound human IgG in the hippocampi, as determined by the mean fluorescence intensity analysis of brain sections, was higher in the NMDAR antibody IgG-injected mice than in healthy control IgG-injected mice in CA1, CA3 and dentate gyrus (DG). (D) For the NMDAR antibody animals ( $n = 5$ ) there was a linear correlation between IgG binding and seizure score ( $R^2 = 0.8$ ;  $P = 0.04$ ). (E) Binding of commercial antibody to an intracellular epitope of the NR1 subunit detected only after permeabilization. (F) Binding of the commercial antibody was not different between NMDAR antibody IgG ( $n = 9$ ) and healthy control IgG ( $n = 7$ ) injected brains. (G). Total surface NMDAR expression in the hippocampus measured by binding of an NMDAR antibody-positive CSF and detected with anti-human IgG; note that the green fluorescence here reflects NMDAR with IgG already bound *in vivo* as well as the CSF NMDAR antibody binding. (H) Total NMDAR, IgG-bound NMDAR on adjacent sections, and non-IgG bound NMDAR. Non-IgG bound NMDAR was calculated by subtracting the IgG-bound fluorescence from that of the total for each pair of sections, and was reduced in the NMDAR antibody IgG-injected mice compared to the healthy control IgG group ( $P = 0.03$ , Mann-Whitney test). Examples are given in Supplementary Fig. 3. IgG binding (green), DPAI binding to nuclei (blue). The data are

presented as mean  $\pm$  SEM. Columns represent results from NMDAR antibody IgG- (red) and healthy control IgG- (blue) injected mice. Numbers below the columns represent (number of brains, number of sections analysed).

**Table 1**  
**Seizure activity following PTZ seizure induction and relationship to IgG bound *in vivo*.**

Animal	IgG injected	Number of stage 2 seizures	Number of stage 3 seizures	Seizure score	Latency to first convulsive seizure (min)	EEG 'spikes' post PTZ	Average fluorescence intensity of IgG bound <i>in vivo</i> (log EC <sub>50</sub> ) (mean ± SEM)	Average fluorescence intensity of IgG bound to CA3 <i>in vivo</i> (log EC <sub>50</sub> ) (mean ± SEM)
E#9	Healthy control subject 1	0	2	6	2.6	4	ND	ND
E#11	NMDAR antibody; Patient 1	0	6	18	1.3	15	ND	ND
E#12	Healthy control subject 1	1	0	2	17.75	0	6.73 ± 0.7	6.51 ± 0.84
E#13	NMDAR antibody; Patient 1	2	6	22	1.3	*Signal loss	ND	ND
E#14	Healthy control subject 1	4	1	11	2.5	14	8.39 ± 0.73	6.58 ± 1.2
E#15	NMDAR antibody; Patient 1	23	10	76	2.3	20	30.18 ± 2.8	37.86 ± 7.1
E#16	Healthy control subject 2	2	0	4	12.3	17	ND	ND
E#17	NMDAR antibody; Patient 2	2	6	22	2.8	6	ND	ND
E#18	NMDAR antibody; Patient 3	9	1	21	6.2	5	ND	ND
E#19	NMDAR antibody; Patient 3	12	3	33	5.3	42	11.1 ± 0.6	11.67 ± 1.1
E#20	NMDAR antibody; Patient 2	18	6	54	1.4	19	8.05 ± 2.1	12.17 ± 6.6
E#21	Healthy control subject 2	5	0	10	15.5	5	5.03 ± 0.4	4.93 ± 0.7
E#22	NMDAR antibody; Patient 2	0	2	6	3.9	*Signal loss	5.57 ± 0.2	5.25 ± 0.21
E#23	NMDAR antibody; Patient 3	2	29	93	0.96	19	36.23 ± 7.1	75.77 ± 17.3
E#24	Healthy control subject 2	3	2	12	2.3	2	6.72 ± 0.69	4.62 ± 0.85

ND=not done.

\* Signal loss denotes that data were unable to be analysed as significant EEG signal fallout during PTZ seizure induction. End-point dilution titres (highest dilution scoring 1 on the range 0–4) of the NMDAR antibody IgG preparations were 1:2000, 1:500 and 1:1500 for Patients 1 and 2 and 3, respectively. The results of IgG bound are taken from the initial experiments. Note that to compare IgG bound *in vivo* with detection of non-IgG bound NMDAR, different sections were used. Those results are summarized in Fig. 3H and illustrated in Supplementary Fig. 3.